Proc. Natl. Acad. Sci. USA
Vol. 95, pp. 691–695, January 1998
Medical Sciences

Rapid noninvasive detection of experimental atherosclerotic lesions with novel ^{99m}Tc-labeled diadenosine tetraphosphates

DAVID R. ELMALEH*†, JAGAT NARULA*‡, JOHN W. BABICH*, ARTIOM PETROV‡, ALAN J. FISCHMAN*, BAN-AN KHAW*‡, ELIEZER RAPAPORT§, AND PAUL C. ZAMECNIK§

*Division of Nuclear Medicine of the Department of Radiology, Massachusetts General Hospital and the Department of Radiology, Harvard Medical School, Boston, MA 02114; ‡Center for Molecular Targeting, Northeastern University, Boston, MA 02210; §Hybridon, Inc., Cambridge, MA 02139; and †Imaging Biopharmaceuticals, Cambridge, MA 02142

Contributed by Paul C. Zamecnik, October 31, 1997

ABSTRACT **The development of a noninvasive imaging procedure for identifying atherosclerotic lesions is extremely important for the clinical management of patients with coronary artery and peripheral vascular disease. Although numerous radiopharmaceuticals have been proposed for this purpose, none has demonstrated the diagnostic accuracy required to replace invasive angiography. In this report, we used the radiolabeled purine analog, ^{99m}Tc diadenosine tetraphosphate (Ap$_4$A; AppppA, P^1,P^4-di(adenosine-5′)-tetraphosphate) and its analogue ^{99m}Tc AppCHClppA for imaging experimental atherosclerotic lesions in New Zealand White rabbits. Serial gamma camera images were obtained after intravenous injection of the radiolabeled dinucleotides. After acquiring the final images, the animals were sacrificed, *ex vivo* images of the aortas were recorded, and biodistribution was measured. ^{99m}Tc-Ap$_4$A and ^{99m}Tc AppCHClppA accumulated rapidly in atherosclerotic abdominal aorta, and lesions were clearly visible within 30 min after injection in all animals that were studied. Both radiopharmaceuticals were retained in the lesions for 3 hr, and the peak lesion to normal vessel ratio was 7.4 to 1. Neither of the purine analogs showed significant accumulation in the abdominal aorta of normal (control) rabbits. The excised aortas showed lesion patterns that were highly correlated with the *in vivo* and *ex vivo* imaging results. The present study demonstrates that purine receptors are up-regulated in experimental atherosclerotic lesions and ^{99m}Tc-labeled purine analogs have potential for rapid noninvasive detection of plaque formation.**

It is becoming increasingly clear that atherosclerosis is an immuno-inflammatory process that involves complex interactions between the vessel wall and blood components (1–5). The atherogenetic process involves sequestration of partially oxidized lipids in the vessel wall (6), which leads to endothelial injury. Endothelial injury promotes adherence of mononuclear cells and platelets that contribute to phenotypic transformation of medial smooth muscle cells (SMCs) from adult to embryonic forms. The transformed muscle cells proliferate and migrate to the intima in parallel with accumulation of lipids by monocytes that leads to the formation of foam cells. Clearly, platelets, macrophages, and proliferating SMCs of atherosclerotic plaque provide important targets for the development of noninvasive diagnostic agents (4–10).

Extra cellular adenine nucleotides are released from a variety of cells and regulate many physiological processes by interaction with P2 purine receptors or adenosine (A1, A2, and A3) receptors (11–14). These compounds can accumulate in atherosclerotic plaque by two mechanisms: (*i*) binding to platelets via interaction with platelet P2T receptors (15), which inhibits platelet aggregation; and (*ii*) binding to P2x and P2y purine receptors on macrophages, monocytes, and SMCs that are present at high concentrations in atherosclerotic lesions.

Recently, it was shown that the adenine analog, Ap$_4$A (AppppA, P^1,P^4-di(adenosine-5′)-tetraphosphate), is ubiquitous in living cells and appears to play an important role in extracellular signaling events in a variety of tissues (11, 12). In particular, this compound was found to be a competitive inhibitor of adenosine diphosphate-induced platelet aggregation (13). Because platelet aggregation plays a central role in arterial thrombosis and plaque formation (10), Ap$_4$A was proposed as a therapeutic agent for inhibition and treatment of plaque formation.

Proliferation of medial SMCs and their migration into vessel intima is an important component of atherogenesis and also occurs in postangioplastic restenosis, allograft-related vasculopathy, and inflammatory vascular conditions such as Kawasaki disease. Proliferation of the SMCs, which represents conversion from adult (contractile) to the neonatal (synthetic) phenotype, is initiated by endothelial damage and is followed by platelet aggregation and release of growth factors. Recently, we used a mouse/human chimeric Z2D3 F(ab)$_2$ specific for the proliferating SMCs of human atheroma for imaging experimental atherosclerotic lesions (16). Because ATP and its analogs are potent inducers of rat aorta medial SMC proliferation in culture, we hypothesized that radiolabeled diadenosine polyphosphates such as Ap$_4$A could be useful reagents for noninvasive imaging of atherosclerotic lesions.

In this report, Ap$_4$A and AppCHClppA (Fig. 1) were labeled with ^{99m}Tc by using glucoheptonate or mannitol as coligand, purified by HPLC, and administered intravenously to New Zealand White rabbits with experimental atherosclerotic lesions. Normal rabbits were used as controls. Serial gamma camera images revealed clear focal areas of increased tracer accumulation in the aortas of all the lesioned animals but none of the controls. These results suggest that ^{99m}Tc-labeled Ap$_4$A and AppCHClppA are potentially useful reagents for rapid noninvasive imaging of atherosclerotic plaque.

MATERIALS AND METHODS

Synthesis of ^{99m}Tc-Ap4A-Glucoheptonate (Mannitol). Fifty to 100 millicuries of $^{99m}TcO_4^-$ obtained from a ^{99} Mo/^{99m}Tc generator (DuPont Merck, Billerica, MA) in 1.5 ml of 0.9% NaCl was used for preparation of a standard glucoheptonate kit (DuPont Merck). Twenty millicuries of ^{99m}Tc-glucoheptonate was added to a solution of 1.0 mg Ap$_4$A (Sigma), and the mixture was stirred for 30 min at room temperature. The reaction mixture was purified by adsorption onto a C$_8$-0DS

Abbreviations: Ap$_4$A, AppppA, P^1,P^4-di(adenosine-5′)-tetraphosphate; SMC, smooth muscle cell; ID, injected dose.

The publication costs of this article were defrayed in part by page charge payment. This article must therefore be hereby marked "*advertisement*" in accordance with 18 U.S.C. §1734 solely to indicate this fact.

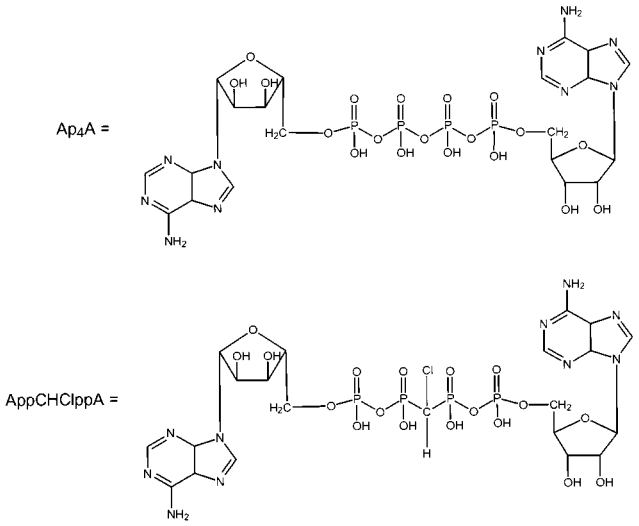

FIG. 1. Chemical structures of Ap_4A and AppCHClppA.

reverse-phase column (5 × 250 mm, Waters) followed by elution with CH_3CN buffer (20:80). The buffer contained 3.1 ml concentrated H_3P0_4 and 3.9 ml t-butylammonium hydroxide, adjusted to pH 2.4 with NaOH. The radioactive peak eluting at 16 min corresponded to ^{99m}Tc-Ap_4A-glucoheptonate and was injected into rabbits as described in the following section. A second radioactive peak eluting at 1–3 min corresponded with ^{99m}Tc-glucoheptonate. The radiochemical yield was 10–30%. Similar results were obtained when Ap_4A was radiolabeled by using ^{99m}Tc-mannitol (17).

Synthesis of ^{99m}Tc-AppCHClppA-Glucoheptonate (or Mannitol). These compounds were prepared exactly as described above by using AppCHClppA.

Experimental Atherosclerotic Lesions. Male New Zealand White rabbits weighing 2.5–3.0 kg (Charles River Breeding Laboratories) were maintained on a 2% cholesterol-6% peanut oil diet (ICN) for 3 months. After 1 week of the hyperlipidemic diet, the abdominal aorta was denuded of endothelium by a modified Baumgartener technique (16). Briefly, each animal was anesthetized with a mixture of ketamine and xylazine (100 mg/ml, 10:1 vol/vol; 1.5–2.5 ml sc), and the right femoral artery was isolated. A 4F Fogarty embolectomy catheter (12–040-4F; Edwards Laboratories, Santa Ana, CA) was introduced through an arteriotomy and advanced under fluoroscopic guidance to the level of the diaphragm. The catheter was inflated to a pressure of 3 psi above the balloon inflation pressure with radiographic contrast media (Conray, Mallinckrodt), and three passes were made down the abdominal aorta with the inflated catheter. The femoral artery then was ligated, and the wound closed. The animals were allowed to recover from anesthesia and then returned to their cages. This protocol was approved by the animal care and use committees of Northeastern University and Massachusetts General Hospital and is in compliance with National Institutes of Health-approved guidelines.

Gamma Camera Imaging of Atherosclerotic and Normal Rabbits. Two to four millicuries of the ^{99m}Tc-Ap_4A-glucoheptonate, ^{99m}Tc-AppCHClppA-glucoheptonate, or ^{99m}Tc-glucoheptonate (control) was injected into marginal ear veins of groups of three rabbits with experimental atherosclerotic lesions. As a control, three unlesioned animals were injected with 2–4 mCi of ^{99m}Tc-Ap_4A-glucoheptonate. After radiopharmaceutical administration, serial gamma images were collected every minute for the first 5 min, every 2 min for the next 25 min, and every 5 min for the next 2.5 hr. In all of the rabbits, images were acquired in the anterior and lateral decubitus projections (including the heart and aorta) by using

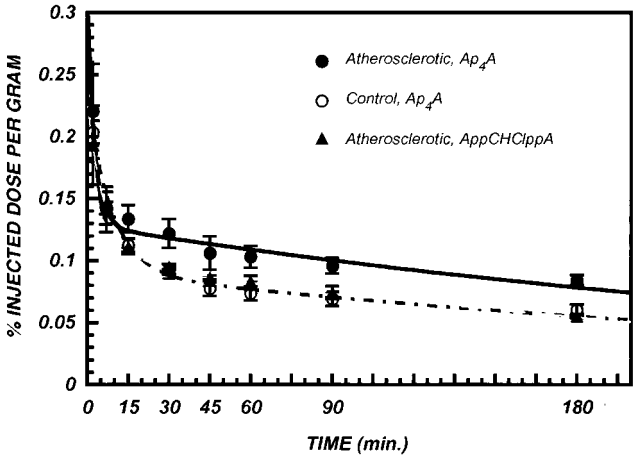

FIG. 2. Blood clearance of ^{99m}Tc-labeled Ap_4A and AppCHClppA in atherosclerotic and control rabbits. The bi-exponential fits to the data are also indicated: ^{99m}Tc-Ap_4A in atherosclerotic rabbits (solid line), ^{99m}Tc-Ap_4A in control rabbits (dot-dashed line), and ^{99m}Tc-AppCHClppA in atherosclerotic rabbits (dashed line). Each point is the mean ± SEM for three animals.

a standard field-of-view gamma camera (Series 100, Ohio Nuclear, Solon, OH) equipped with a high-resolution parallel-hole collimator and interfaced with a dedicated computer system (Technicare 560, Solon, OH). The pulse height analyzer was adjusted to record the 140 KeV photopeak of ^{99m}Tc, and all images were recorded in a 256 × 256 matrix.

After acquiring the final images, the animals were sacrificed with an overdose of sodium pentobarbital. The aortas were removed, opened along the ventral surface, and mounted on styrofoam blocks. The aortas then were placed on the face of the gamma camera and *ex vivo* images were recorded (10 min).

Blood Clearance of ^{99m}Tc-Ap_4A. Blood samples (0.1 ml) were withdrawn in parallel with the imaging studies in atherosclerotic and control rabbits and radioactivity was measured with a well-type gamma counter (LKB model 1282, Wallac Oy, Finland). To correct for decay and permit calculation of the concentration of radioactivity as a fraction of the administered dose, aliquots of the injected doses (IDs) were counted simultaneously. Blood radioactivity [% ID/g] was plotted as a function of time after injection, and the curves were fitted to bi-exponential functions.

Biodistribution. After acquiring the *ex vivo* images, biodistribution was measured. Samples of blood, heart, lung, liver, spleen, kidney, skeletal muscle, normal aorta, and lesioned aorta were washed with saline, weighed and radioactivity was measured with a well type gamma counter (LKB model 1282). To correct for radioactive decay and permit calculation of the

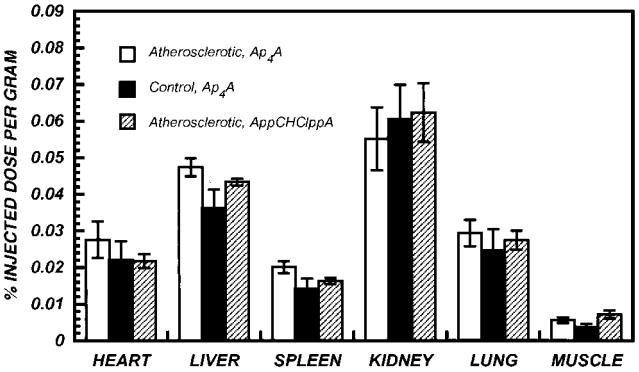

FIG. 3. Biodistribution of ^{99m}Tc-Ap_4A-glucoheptonate in nontarget organs at 3 hr after administration. Each bar is the mean ± SEM for three animals.

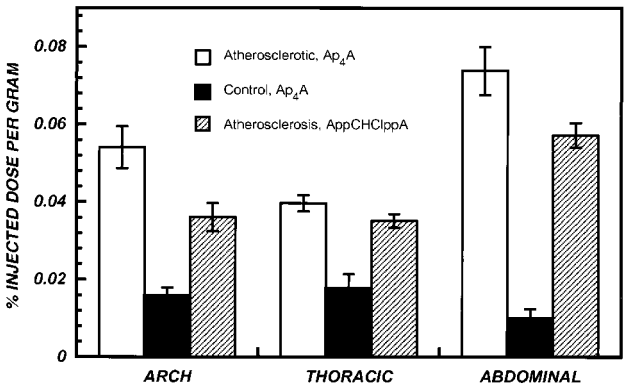

FIG. 4. Accumulation of ^{99m}Tc-labeled Ap_4A and AppCHClppA in lesioned and normal aortic segments of rabbits at 3 hr after i.v. administration. Each bar is the mean ± SEM for three animals.

concentration of radioactivity in each organ as a fraction of the administered dose, aliquots of the IDs were counted simultaneously. The results were expressed as % ID/g.

Statistical Methods. The results were evaluated by one-way ANOVA followed by Duncan's New Multiple Range Test. The blood clearance curves were fitted to bi-exponential functions by nonlinear least squares.

RESULTS

Radiochemistry. The method for radiolabeling Ap_4A described here resulted in a purer and more consistent product than a previously reported procedure (18). This procedure described above that used glucoheptonate as the coligand yielded a mixture of the ^{99m}Tc-glucoheptonate (retention time 2–3 min, see above) and ^{99m}Tc-Ap_4A-glucoheptonate at 16 min. With this procedure, ^{99m}Tc-Ap_4A-glucoheptonate was isolated with a radiochemical purity of >90%. Similar results were obtained when ^{99m}Tc-mannitol was used as the coligand.

Blood Clearance of ^{99m}Tc-Ap_4A. Blood clearance of the ^{99m}Tc-Ap_4A-glucoheptonate was rapid. In the control rabbits, the concentration of radioactivity (% ID/g) in the circulation averaged 0.25% at 2 min, after injection, decreased to 0.08% ID/g at 60 min and only slightly thereafter (up to 180 min). For all groups of rabbits, blood clearance was well described by bi-exponential functions with fast and slow components ($t_{1/2}$s) of ≈4 and ≈ 250 min, respectively (Fig. 2). Blood clearance was not significantly different between rabbits with atherosclerotic lesions and controls.

Biodistribution in Nontarget Organs. The biodistribution of ^{99m}Tc-Ap_4A-glucoheptonate in nontarget organs at 3 hr after injection is summarized in Fig. 3. Overall, these data clearly demonstrate that accumulation (% ID/g) of the radiopharmaceuticals in normal tissues was quite low: heart (0.02%), liver (0.04%), lung (0.02%), kidney (0.06%), and spleen (0.1%). The degree of tracer accumulation by the different tissues was statistically significant ($P < 0.01$). However, concentrations were similar for all radiopharmaceuticals (P = NS). Of all the tissues that were sampled, kidney contained the highest concentration of tracer ($P < 0.01$). Liver and lung had higher concentrations than spleen and muscle ($P < 0.05$), and spleen had higher concentration compared with muscle ($P < 0.05$).

^{99m}Tc (Coligand)-Ap_4A Accumulation in Atherosclerotic Lesions. Fig. 4 summarizes the concentrations of radioactivity in lesioned and normal aortic segments of rabbits at 3 hr after i.v. administration of both ^{99m}Tc (coligand)-Ap_4A analogs. The mean % ID/g of ^{99m}Tc (coligand)-Ap_4A in the lesioned segments was higher than the background activity in the normal specimens: 0.074% vs. 0.01% ($P < 0.01$). Aortic arch segments (which were not denuded) showed slightly greater accumulation of ^{99m}Tc-Ap_4A analogs comparable to thoracic segments.

When the data were expressed at lesioned/normal rations, accumulation of ^{99m}Tc (coligand)-Ap_4A in atherosclerotic lesions of balloon-denuded (abdominal) aorta was 7.4-fold greater than in uninjured (abdominal) aorta of control rabbits and ≈2-fold greater than the unlesioned thoracic segments of aortas of rabbits with abdominal lesions. As the results in Table 1 indicate, focal regions of tracer accumulation were detected in aortic segments of all lesioned rabbits imaged with either Ap_4A or AppCHClppA but in none of the controls. Although accumulation in atherosclerotic lesions was slightly greater for Ap_4A compared with AppCHClppA, the difference was not statistically significant.

Gamma Camera Imaging. All of the rabbits with experimental atherosclerosis showed rapid accumulation of radioactivity in the lesioned areas; representative images are shown in Fig. 5. The lesions were clearly visible within 20 min after injection, and radioactivity was retained in the lesions for the full 3 hr of the imaging session. When the aortas were imaged *ex vivo*, the pattern of radioactivity distribution closely paralleled the imaging results (Fig. 5). Inspection of the excised aortas revealed lesion patterns that were virtually identical to the results of *in vivo* and *ex vivo* imaging (Fig. 5). In contrast, both *in vivo* and *ex vivo* gamma camera imaging failed to demonstrate evidence of focal tracer accumulation in aortas of unlesioned rabbits; representative images are shown in Fig. 6. Inspection of the aortic specimens showed no evidence of vessel damage. Imaging atherosclerotic rabbits with ^{99m}Tc-labeled glucoheptonate showed no evidence of specific accumulation in the aortic lesions, and the images were indistinguishable from those obtained in control rabbits imaged with ^{99m}Tc-labeled Ap_4A or AppCHClppA (data not shown). With this tracer, radioactivity cleared rapidly from all organs ($t_{1/2}$s: ≈5–10 min) and accumulated in the kidneys and bladder.

DISCUSSION

The development of a noninvasive test for identifying metabolically active lesions should provide information on the pathogenesis of atherosclerotic plaque formation. With such a procedure it might be possible to detect "vulnerable" lesions before they become unstable and lead to subintimal hemorrhage and coronary occlusion or clinical manifestations such as ischemia. In addition, a noninvasive test of this type could be important not only for diagnosis but also for development

Table 1. Accumulation of ^{99m}Tc-labeled Ap_4A and AppCHClppA in lesioned and control aortic segments

Tracer	No.	Condition	Lesion visualization	% ID/gram	
				Abdominal aorta	Thoracic aorta
Ap_4A	3	Atherosclerotic	3/3	0.074 ± 0.01*	0.040 ± 0.004
AppCHClppA	3	Atherosclerotic	3/3	0.060 ± 0.007*	0.030 ± 0.001
Ap_4A	3	Control	0/3	0.010 ± 0.004	0.016 ± 0.006

*P = 0.003.

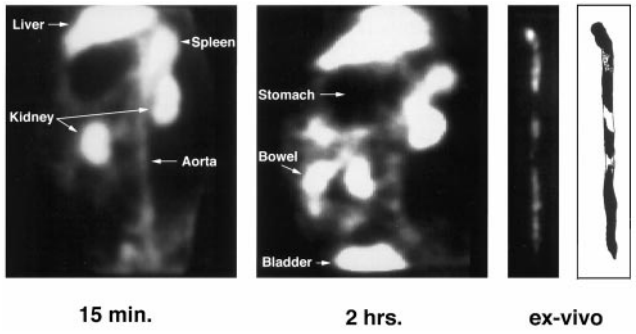

FIG. 5. Images of the aorta of a rabbit with experimental atherosclerosis. *In vivo* gamma camera images (lateral decubitus projection) acquired at 15 min (*Left*) and 2 hr (*Center*) after injection of ^{99m}Tc-Ap$_4$A. (*Right*) Corresponding *ex vivo* gamma camera image and sketch of the lesioned areas.

and monitoring of therapies directed at altering the natural history of these lesions. There are a limited number of reports describing noninvasive visualization of atherosclerotic lesions. These studies have targeted the thrombotic component overlying the atherosclerotic lesion (with radiolabeled fibrinogen) (19, 20) platelet aggregation at regions of turbulent flow (with labeled platelets or platelet-specific antibodies) (21–23) or proteins likely to be incorporated into atherosclerotic lesions (with radiolabeled autologous lipoproteins) (24–29). Nonspecific uptake of human IgG via Fc receptors of macrophages also has been used as the basis for a targeting strategy (2, 30, 31). More recently, the Fab′ fragment of a monoclonal IgM antibody, Z2D3, which is directed to an antigen associated with the proliferating SMCs of human atherosclerotic lesions showed rapid accumulation and good localization of lesions in an experimental model (16).

Ap$_4$A undergoes rapid degradation in the vascular bed by the catalytic actions of ecto and phosphodiesterases and soluble nucleotide pyrophosphates. We have demonstrated, however, that the ^{99m}Tc-chelates of Ap$_4$A and its analog are much more stable *in vivo* compared with the corresponding sodium salts (data not shown).

In the current study, ^{99m}Tc-Ap$_4$A-glucoheptonate and its analog accumulated rapidly in atherosclerotic lesions and were retained for more than 3 hr. At 1 hr after injection, lesion to blood radioactivity ratios were greater than 6 to 1. The ^{99m}Tc-Ap$_4$A analogs showed very low levels of accumulation in normal tissues of the rabbit. When ^{99m}Tc-glucoheptonate (control) was injected in lesioned animals, very low concentrations of radioactivity accumulated in atherosclerotic lesions and normal tissues. Similarly, very low levels of ^{99m}Tc-Ap$_4$A and its analog accumulated in the tissues of uninjured (control) animals. Thus, we have demonstrated the feasibility of rapid noninvasive imaging of

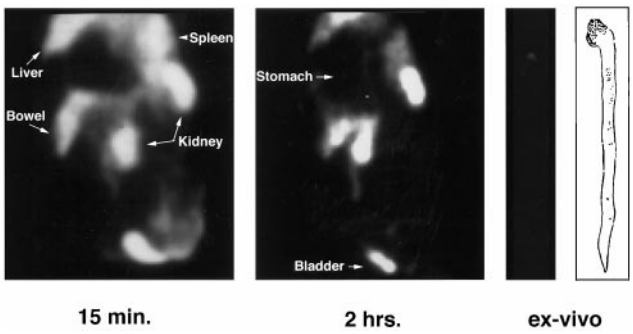

FIG. 6. Images of the aorta of a control rabbit. *In vivo* gamma camera image acquired at 15 min (*Left*) and 2 hr (*Center*) after injection of ^{99m}Tc-Ap$_4$A-glucoheptonate. (*Right*) Corresponding *ex vivo* gamma camera image and sketch of the lesioned areas.

experimentally induced atherosclerotic lesions with radiolabeled ^{99m}Tc-Ap$_4$A analogs. In all cases, lesion visualization was possible within 15–30 min after tracer administration.

In addition to demonstrating the feasibility of using this class of reagents for scintigraphic localization of atherosclerotic lesions, our results provide indirect evidence for up-regulation of purinoreceptors in atherosclerotic plaques and could help to unravel an important mechanism of atherogenesis. The role of surface receptors coupled with intrinsic tyrosine kinase activity has been extensively studied in proliferating SMCs of atheroma but the role of G protein-coupled receptors has not been described. SMCs isolated from human and rat aorta, which acquire synthetic phenotypic characteristics in tissue culture, proliferate rapidly and show high intracellular Ca^{2+} content in response to extracellular ATP. The mitogenic and Ca^{2+} mobilizing effects of diadenosine polyphosphates are as potent as ATP (16). The present study provides an *in vivo* characterization of purinoreceptors. Determination of the precise cellular and subcellular site(s) of tracer binding within the atherosclerotic lesions was beyond the scope of the present investigations and awaits the results of future microautoradiographic studies with ^{95m}Tc- or ^{1}H-labeled agents.

Although angiography is the "gold standard" for measuring luminal narrowing and has been useful for monitoring therapeutic interventions, it is of limited value for evaluating early lesions. For optimal care of atherosclerotic disease, characterization of plaque constituents and metabolism is imperative. With this information it may be possible to differentiate stable plaques from those in which rupture or encroachment on the lumen are imminent. Thus, quantitation of concentration of foam cells, SMC proliferation, and amount of overlying thrombotic plaque could have significant impact in assessing prognosis.

Several clinical vasculopathies such as restenotic complications of angioplasty and allograft-related vasculopathy are associated with rapid proliferation of SMCs; however, no diagnostic or prognostic strategies have provided enough information for early intervention in these patients. Recently the Fab′ fragment of an antibody, Z2D3, which is specific for a surface antigen of SMCs with the synthetic phenotype was shown to be useful for rapid detection of experimental atherosclerotic lesions (16). The results of the current study indicate that ^{99m}Tc-Ap4A analogs accumulate in experimental lesions even more rapidly than Z2D3.

CONCLUSIONS

The present study demonstrates that ^{99m}Tc-labeled adenine nucleotide analogs (Ap$_4$A and AppCHClppA) that are stable *in vitro* and *in vivo* are easily prepared in high yield and purity. The competitive inhibition of Ap$_4$A and AppCHClppA at ADP association sites on platelets makes them potentially highly selective pharmacological agents for vascular lesions where platelets show early localization and aggregation. These radiopharmaceuticals have potential both as radiodiagnostic agents for the rapid detection of atherosclerotic plaques and for probing the fundamental pathophysiology of atherogenesis.

We thank Dr. Barry Zaret for his review and constructive comments on this manuscript.

1. Ross, R. (1986) *N. Engl. J. Med.* **314,** 488–500.
2. Hathaway, D. R. & March, K. L. (1989) *J. Am. Coll. Cardiol.* **13,** 265–282.
3. Fuster, V., Badimon, L., Badimon, J. J. & Chesebro, J. H. (1992) *N. Engl. J. Med.* **326,** 242–250.
4. Davies, M. J. & Woolf, N. (1993) *Br. Heart J.* **69,** Suppl., S3–11.
5. Narula, J., Ditlow, C., Chen, F. W. & Khaw, B. A. (1994) in *Monoclonal Antibodies in Cardiovascular Diseases*, eds. Khaw, B. A., Narula, J. & Strauss, H. W. (Lea & Febiger, Philadelphia), pp. 206–215.

6. Witztum, J. L. & Steinberg, D. (1991) *J. Clin. Invest.* **88,** 1785–1792.
7. Butcher, E. C. (1991) *Cell* **67,** 1033–1036.
8. Thyberg, J., Heidin, U., Sjolund, M., Palmberg, L. & Bottger, B. A. (1990) *Arteriosclerosis* **10,** 966–990.
9. Grotendorst, G. R., Seppa, H. E. J., Kleinman, H. K. & Martin, G. R. (1981) *Proc. Natl. Acad Sci. USA* **78,** 3669–36672.
10. Khaw, B. A., Carrio, J. & Narula, J. (1995) in *Handbook of Target Delivery of Imaging Agents*, ed. Torchilin, V. (CRC, Boca Raton, FL), pp. 429–443.
11. Zamecnik, P. C. & Stephenson, M. L. (1969) in *Alfred Benzon Symposium I: The Role of Nucleotides for the Function and Conformation of Enzymes*, eds Kalckar, H. M., Klenow, H., Munch-Peterson, A., Ottesen, M. & Thaysen, J. M. (Munksgaard, Copenhagen), pp. 276–291.
12. Rapaport, E. & Zamecnik, P. C. (1976) *Proc. Natl. Acad. Sci. USA* **73,** 3984–3988.
13. Zamecnik, P. C., Kim, B., Guo, M. J., Taylor, G. & Blackburn, G. M. (1992) *Proc. Natl. Acad. Sci. USA* **89,** 2370–2373.
14. Kim, B. K., Zamecnik, P., Taylor, G., Guo, M. J. & Blackburn, G. M. (1992) *Proc. Natl. Acad. Sci. USA* **89,** 11056–11058.
15. Chan, S. W., Gallo, S. J., Kim, B. K., Guo, M. J., Blackburn, G. M. & Zamecnik, P. C. (1997) *Proc. Natl. Acad. Sci. USA* **94,** 4034–4039.
16. Narula, J., Petrov, A., Bianchi, C., Ditlow, C. C., Lister, B. C., Dilley, J., Pieslak, B., Chen, W. F., Torchilin, V. P. & Khaw, B. A. (1995) *Circulation* **92,** 474–484.
17. Babich, J. W. & Fischman, A. J. (1995) *Nuclear Med. Biol.* **22,** 25–30.
18. Elmaleh, D. R., Zamecnik, P. C., Castronovo, F. P., Strauss, H. W. & Rapaport, E. (1984) *Proc. Natl. Acad. Sci. USA* **81,** 918–921.
19. Mettinger, K. L., Ericson, K., Larsson, S. & Casseborn, S. (1978) *Lancet* **1,** 242–244.
20. Ord, J. M., Hasapes, J., Daugherty, A., Thorpe, S. R., Bergmann, S. R. & Sobel B. E. (1992) *Circulation* **85,** 288–297.
21. Davis, H. H., Siegel, B. A., Joist, J. H., Heaton, W. A., Mathias, C. J., Sherman, L. A. & Welch, M. J. (1978) *Lancet* **1,** 1185–1187.
22. Davis, H. H., Siegel, B. A., Sherman, L. A., Heaton, W. A., Naidich, T. P., Joist, J. H. & Welch, M. J. (1980) *Circulation* **61,** 982–988.
23. Minar, E., Ehnnger, H., Dudczak, R., Schofl, R., Jung, M., Koppensteiner, R., Ahmadi R. & Kretschmer, G. (1989) *Stroke* **20,** 27–33.
24. Roberts, A. B., Lees, A. M., Lees, R. S., Strauss, H. W., Fallon, J. T., Taveras, J. & Kopiwoda, S. (1983) *J. Lipid Res.* **24,** 1160–1167.
25. Isaacsohn, J. L., Lees, A. M., Lees, R. S., Strauss, H. W., Barlai-Kovach, M. & Moore, R. J. (1986) *Metabolism* **35,** 364–366.
26. Moerlein, S. M., Daugherty, A., Sobel, B. E. & Welch, M. J. (1991) *J. Nucl. Med.* **32,** 300–307.
27. Lees, R. S., Lees, A. M. & Strauss, H. W. (1983) *J. Nucl. Med.* **24,** 154–156.
28. Lees, A. M., Lees, R. S., Schoen, F. J., Isaacsohn, J. L., Fischman, A. J., McKusick, K. A. & Strauss, H. W. (1988) *Arteriosclerosis* **8,** 461–470.
29. Ginsberg, H. N., Goldsmith, S. J. & Vallabhajosula, S. (1990) *Artenosclerosis* **10,** 256–262.
30. Fischman, A. J., Rubin, R. H., Khaw, B. A., Kramer, P. B., Wilkinson, R. A., Ahmad, M., Needelman, M., Locke, E., Nossiff, N. D. & Strauss, H. W. (1989) *J. Nucl. Med.* **30,** 1095–1100.
31. Fischman, A. J., Rubin, R. H., Delvecchio, A., Ahmad, M., Khaw, B. A., Callahan, R. J., LaMuraglia, G. M. & Strauss, H. W. (1989) *J. Nucl. Med.* **30,** 817.